NANO LETTERS

2007
Vol. 7, No. 9
2753−2757

Moving Nanoparticles with Raman Scattering

M. Ringler,[†] T. A. Klar,[*,†] A. Schwemer,[†] A. S. Susha,[†] J. Stehr,[†] G. Raschke,[†] S. Funk,[†] M. Borowski,[†] A. Nichtl,[‡] K. Kürzinger,[‡] R. T. Phillips,[§] and J. Feldmann[†]

Photonics and Optoelectronics Group, Physics Department and CeNS, Ludwig-Maximilians-Universität München, Amalienstrasse 54, 80799 Munich, Germany, Roche Diagnostics GmbH, Nonnenwald 2, 82372 Penzberg, Germany, and Cavendish Laboratory, University of Cambridge, J J Thomson Avenue, Cambridge CB3 0HE, United Kingdom

Received May 25, 2007; Revised Manuscript Received July 18, 2007

ABSTRACT

We show how to change optically the distance between two protein-linked gold nanoparticles by Raman-induced motion of the linker protein. Rayleigh scattering spectroscopy of the coupled-particle plasmon allows us to compare the inter-nanoparticle distance of individual protein-linked gold nanoparticle dimers before and after surface-enhanced Raman scattering (SERS). We find that low-intensity (50 μW/μm^2) laser light in resonance with the nanoparticle-dimer plasmon provokes a change of the inter-nanoparticle distance on the order of 0.5 nm whenever SERS from the proteins connecting the nanoparticles can be observed.

Metallic nanostructures increase Raman signals by a factor of up to 10^{14},[1−3] making surface-enhanced Raman scattering (SERS) a highly sensitive and selective detection method for nucleic acids,[4,5] for proteins,[6,7] and even for single molecules.[8,9] Significant transfer of ground state population to excited vibrational states of SERS-active molecules has been reported.[10] While chemical enhancement also contributes,[11] the main cause of the SERS effect is the enhancement of the local electric field at hot spots of a nanostructured substrate.[12,13] Hot spots arise where localized nanoparticle plasmons couple to each other. The simplest system, in which this coupling of plasmons can be studied, is a dimer of two spherical gold nanoparticles of equal size (Figure 1a). Here, the nanoparticle plasmons couple strongly and a hot spot arises in the interparticle gap if the polarization of the incident light is in line with the dimer axis. A SERS effect has been observed for this polarization.[7,14,15]

Previous studies have focused on how SERS depends on the hot spot. In contrast, we show in this report that Raman-active molecules can act back on the hot spot, pushing the nanoparticles apart or pulling them together. Such a change of the inter-nanoparticle distance can be accurately measured by Rayleigh-scattering spectroscopy because even sub-nanometer variations in the interparticle distance cause a substantial spectral shift of the coupled nanoparticle plasmon.[16,17] We show, using Rayleigh and Raman spectroscopy of single nanoparticle dimers, that the interaction between the molecule and the hot spot eventually drives the dimer into a configuration where the hot spot Rayleigh resonance is spectrally detuned from the Raman laser.

We produce nanoparticle dimers by linking biotin-functionalized gold nanoparticles with streptavidin (SA) as illustrated in Figure 1b. Gold nanoparticles with a diameter of 40 nm are coated with biotinylated bovine serum albumin (BSA-Bi). We add 150 streptavidin molecules per nanoparticle and allow clusters of nanoparticles to form over several hours. Electrostatic repulsion between the nanoparticles is suppressed by incubating at pH 5.5 where the zeta potential is reduced to $\zeta = -7.0 \pm 0.8$ mV (from $\zeta = -26.4 \pm 0.3$ mV at neutral pH). Submarine agarose gel electrophoresis is used to analyze and purify the sample. The inset of Figure 1c shows a photograph of the gel. In the left lane, the sample containing biotinylated nanoparticles and streptavidin has separated into three bands corresponding to monomers, dimers, and larger multimers. In the right lane, a control sample without streptavidin migrates as a single band toward the positive electrode, confirming that the clusters are indeed linked by streptavidin as illustrated in Figure 1b.

After electrophoresis, the dimer band (indicated by an arrow) is excised and the nanostructures are retrieved from the gel by electroelution. Transmission electron micrographs like the one in Figure 1c show that the sample consists mostly of dimers (about two-thirds of the particles, the rest occurring as monomers). Electron microscopy at higher magnification (as in Figure 1d) confirms that the particles are almost

[†] Ludwig-Maximilians-Universität München.
[‡] Roche Diagnostics GmbH.
[§] University of Cambridge.

10.1021/nl0712466 CCC: $37.00
Published on Web 08/14/2007

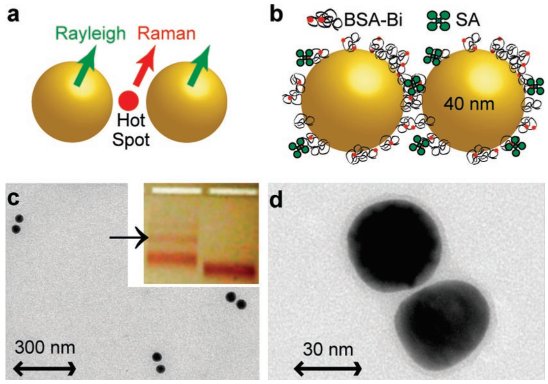

Figure 1. (a) A noble metal nanoparticle dimer encloses an interstitial hot spot where surface-enhanced Raman scattering can occur. The Rayleigh scattering spectrum contains information about the inter-nanoparticle distance. **(**b**)** Experimental realization of scheme (a). Gold nanoparticles (40 nm) coated with biotinylated bovine serum albumin (BSA-Bi) are linked together by streptavidin (SA). **(**c**)** After synthesis, the dimers are purified by gel electrophoresis (inset, left lane). Three red bands are discernible, which originate from single particles with streptavidin, dimers (→), and clusters of more than two particles, respectively. The biotinylated nanoparticles without streptavidin (right lane) migrate in a single band slightly faster than the monomers with streptavidin, probably due to their smaller effective radius. Transmission electron microscopy of a sample extracted from the second band of the left lane shows that this band consists mostly of dimers. The interparticle distance varies from <1 to 13 nm. No touching particles are found. **(**d**)** Higher magnification TEM micrograph of a typical nanoparticle dimer. The particles are spherical with a diameter of 40 nm.

spherical and uniform in size and allows us to determine precisely the interparticle distances. We find that the interparticle distances are broadly distributed from about 0.5 nm to an upper limit of about 13 nm. Particles touching each other without any gap are not observed. The maximum distance of 13 nm corresponds to the length of a fully stretched BSA-Bi−streptavidin−Bi-BSA linker. Dimers with smaller distances have an angled linker configuration.

The sample is investigated with a microscope setup that allows us to measure consecutively Raman and Rayleigh scattering spectra of the same nanometer-sized object with short switching delays (Figure 2a). For Rayleigh scattering measurements, white light from a 100 W halogen lamp is focused at large angles onto the sample using a dark-field condenser with high numerical aperture (NA = 1.2−1.4). As depicted in Figure 2a, the scattered light from a single nanoparticle dimer in focus is collected by a water immersion objective lens (100×, NA = 1.0) and then polarization analyzed before being spectrally resolved in a grating spectrometer and detected with a nitrogen-cooled, back-illuminated CCD camera.[18] For Raman scattering measurements, light from a He−Ne laser is passed through a 632.8 nm laser-line filter. The polarization of the laser beam can be adjusted with a $\lambda/2$ plate. The laser is coupled into the microscope with a nonpolarizing beam splitter. The Raman signal is collected with the same spectrometer and CCD as the Rayleigh signal except that the polarization analyzer is replaced by a long-pass edge filter that transmits the Raman−Stokes signal and blocks resonantly scattered laser light.

Rayleigh spectroscopy permits detection of changes in the distance between the gold nanoparticles with high sensitivity. Two orthogonal plasmonic resonances are excited by light polarized along the dimer axis and perpendicular to it. When the field vector $\mathbf{E}$ is perpendicular to the dimer axis $\mathbf{d}$, the scattering spectrum features a maximum whose frequency is very close to that of the single-particle plasmon. When $\mathbf{E}$ is parallel to $\mathbf{d}$, the scattering peak is red-shifted compared to the single-particle plasmon. Rayleigh spectra of three different gold nanoparticle dimers are shown in the upper part of Figure 2b. The closer the nanoparticles are, the stronger is the coupling between their plasmon oscillations and therefore the larger is the splitting between the two resonances. In order to deduce quantitatively the interparticle distance $d = |\mathbf{d}|$ of the dimers from their Rayleigh scattering spectra, we compare the measured resonance positions with

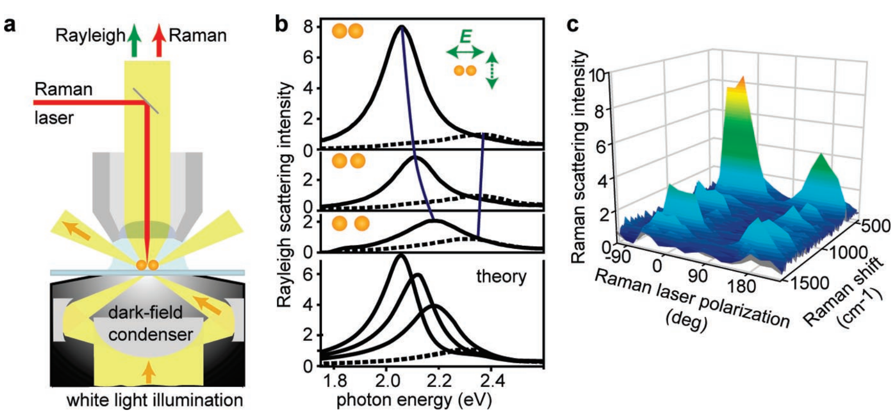

Figure 2. (a) Experimental setup. A transmission mode dark-field microscope is combined with an epi-illumination Raman setup. Thus, Raman and Rayleigh scattering spectra can be observed for one and the same gold nanoparticle dimer. **(**b**)** Experimental Rayleigh scattering spectra from nanoparticle dimers at **E**-field polarizations parallel (solid lines) and perpendicular (dashed) to the dimer axis, in comparison with calculated scattering cross sections (lowest panel). Strong coupling between the nanoparticle plasmons leads to a large energy splitting between the orthogonal Rayleigh modes, and the coupling is the stronger the closer the nanoparticles are. Therefore large energy differences correspond to small distances and vice versa. In this way, the Rayleigh scattering spectrum is indicative of the dimer geometry and in particular, the interparticle distance. Comparison of the experimental and theoretical results yields experimental distances of 2, 3, and 6 nm for the three measured spectra (top to bottom). **(**c**)** Typical polarization-dependent Raman spectra. Raman scattering is strong when the polarization of the exciting laser is parallel to the dimer axis (0° and 180°)−leading to strong field enhancement in the interparticle gap−and is absent for perpendicular polarization.

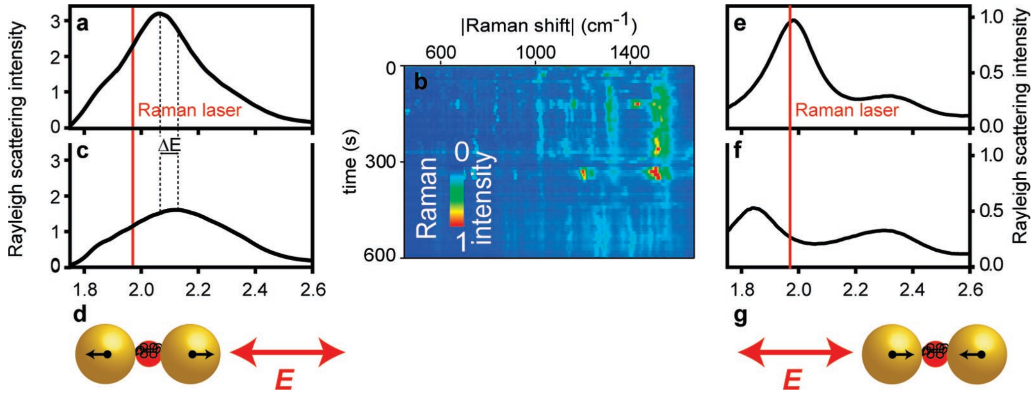

Figure 3. Moving nanoparticles with Raman scattering. **(**a**)** The initial on-axis Rayleigh scattering resonance of a nanoparticle dimer corresponding to an inter-nanoparticle distance of 2.3 nm. **(**b**)** The dimer from (a) is exposed to laser illumination with the frequency indicated by the red line in (a) and polarization as shown in (d). The initially strong SERS signal becomes faint after ~6 min. **(**c**)** The particles have moved apart by 1 nm, which becomes apparent as a blue-shift of the on-axis dimer resonance by $\Delta E = 50$ meV. **(**e and f**)** A different dimer ($d = 1.1$ nm), where the particles move closer by 0.6 nm as can be deduced from a red shift of the resonance by $\Delta E = 130$ meV. Both in (a)−(c) and (e) and (f) the plasmon peak has become detuned from the exciting laser frequency. Therefore the SERS effect is weaker, which explains the diminishing Raman signal. **(**d and g**)** Graphical illustrations of the motion of the nanoparticles in both cases.

calculations[16] shown in the lower part of Figure 2b. For small d the dependence of the low-energy resonance frequency on the particle-to-particle distance is very steep ($dE/dd = 16$ meV/Å at $d = 1$ nm), which allows us to detect distance changes in the angstrom range likely to go unnoticed when Raman microscopy is combined with atomic force microscopy or scanning electron microscopy.[15,19] This holds true even when there are higher order resonances in the longitudinal-mode dimer scattering spectrum. Such higher order resonances have been calculated in ref 20 and experimentally observed in ref 21.

With the same setup that allows us to measure Rayleigh scattering, we can also observe Raman scattering from the inter-nanoparticle hot spot. The fact that the Raman signal does indeed originate in the hot spot becomes apparent in the polarization dependence of the Raman intensity shown in Figure 2c. We see that the Raman signal is maximal when light field **E** and interparticle axis **d** are aligned (0° and 180°), since this is the situation where there is a strongly enhanced electric field in the interparticle gap;[14] the Raman signal is lowest when **E** is orthogonal to **d** (90°), and the field enhancement is comparatively small.

Now we combine the Rayleigh and Raman techniques. First, Rayleigh spectra are measured to obtain the initial distance and orientation of the dimer. Then, the dimer is exposed to laser light of moderate intensity ($\leq 100\ \mu W/\mu m^2$), which is polarized along the interparticle axis **d**, and Raman spectra are collected. Finally, another Rayleigh spectrum is recorded under white-light illumination.

Illustrative data are shown in parts a−c of Figure 3. Before exposure to the Raman laser, the on-axis Rayleigh scattering spectrum peaks at 2.07 eV (Figure 3A), which corresponds to an interparticle distance of 2.3 nm. Then the dimer is exposed to light from the 632.8 nm line of a He−Ne laser for 10 min, and Raman scattering is measured (Figure 3b). SERS signals from the hot spot, shown in Figure 3B, fluctuate in intensity and spectral position and become faint after about 6 min. The fluctuations have been attributed to movement of the Raman-active molecules through the hot spot, to charge transfer, and to various other mechanisms.[19,22] The possibility that the Raman process itself can change the hot spot that favors it has not been considered, since this effect cannot be detected by measurement of Raman scattering alone. However, the Rayleigh scattering spectrum after SERS in Figure 3c shows clear evidence for such a process. The scattering peak has blue-shifted to 2.12 eV, which corresponds to an increased interparticle distance d of 3.3 nm.

In the sequence shown in parts a−c of Figure 3 the interparticle distance d has increased after Raman scattering. We also observed dimers where d decreases and the plasmon shifts to lower energy. One example is shown in parts e and f of Figure 3 where the distance decreased from 1.1 nm (Figure 3e) to 0.4 nm (Figure 3f). The extent and direction of the shift varies from dimer to dimer. However, the detuning of the on-axis-plasmon from the spectral position of the Raman laser is a general pattern observed in all cases where a Raman signal is detected. The polarization dependence of the Rayleigh scattering spectra always remains unchanged, which means that the orientation of the dimer axis always remains fixed in space.

In some cases, a dimer does not show a Raman signal when exposed to light polarized along its axis. Such a case is depicted in parts a−c of Figure 4. Again we start by measuring a Rayleigh scattering spectrum for the on-axis polarization (Figure 4a) and proceed by exposing the dimer to Raman laser light polarized along the interparticle axis. However, in contrast to the situation in Figure 3b, no SERS signal is observed (Figure 4b). After a collection time of 1000 s, we switch off the Raman laser to measure a postexposure Rayleigh spectrum. In this case the Rayleigh spectrum after exposure to the Raman laser (Figure 4c) is identical to the Rayleigh spectrum before exposure (Figure 4a). The crucial point is that in all the cases, where no Raman scattering is observed, we do not observe a spectral shift in the Rayleigh scattering spectra either. In contrast, the

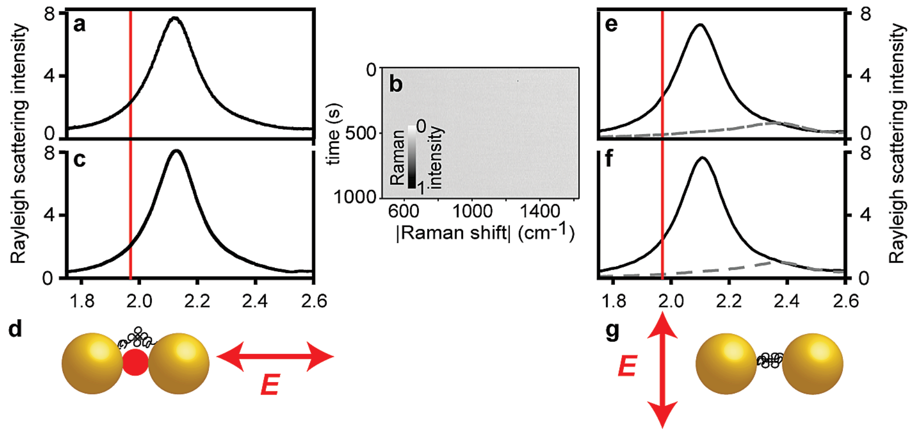

Figure 4. The inter-nanoparticle distance remains constant when no Raman emission is observed. **(a)** The initial on-axis Rayleigh scattering resonance of a nanoparticle dimer (d = 3.8 nm). **(b)** The dimer is illuminated with laser light polarized along the interparticle axis, such that an interparticle hot spot forms. However, no SERS signal is observed. **(c)** The Rayleigh spectrum after exposure to the Raman laser is unchanged with respect to A. **(d)** The lack of Raman scattering and induced distance change can be explained with the assumption that the linker protein is situated outside the SERS hot spot. **(e)** and **(f)** Rayleigh scattering spectra from another dimer (d = 3.6 nm). In this case the Raman laser is polarized perpendicular to the interparticle axis. Therefore, it excites the high-energy plasmon resonance shown as a dashed line in the initial Rayleigh spectrum. No SERS signal is observed, and the Rayleigh scattering spectrum is not affected by exposure to the Raman laser. **(g)** Here, the lack of Raman scattering and induced distance change is due to the fact that no hot spot forms for this polarization of the incident field.

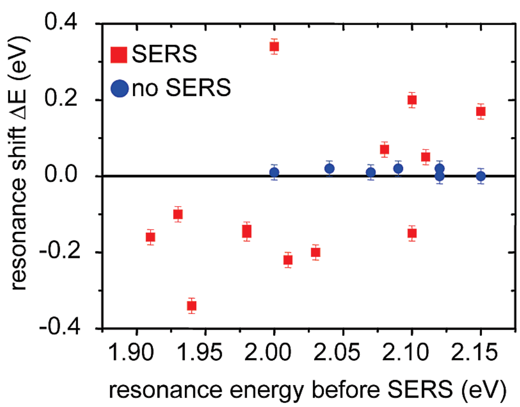

Figure 5. Shift of the longitudinal-mode Rayleigh scattering resonance energy ΔE vs initial resonance energy. Data points from dimers that show SERS are represented as red squares, those from dimers that do not show SERS are show as blue circles. A strong correlation between SERS activity and change of the resonance energy becomes apparent: dimers with SERS show a resonance shift, dimers with no detectable SERS do not.

interparticle distance changes noticeably when a dimer does show SERS. In Figure 5 the shift of the resonance energy ΔE is plotted against the initial resonance energy for the two groups of dimers. The graph shows an almost perfect correlation between the detection of a Raman signal and a change of the dimer distance that detunes the nanostructure resonance with respect to the Raman laser. We conclude that the Raman excitation of the vibrational degrees of freedom of the protein eventually leads to changes in its conformation which concomitantly change the distance of the metal nanoparticles by up to a nanometer.

Considering the typical long-term evolution of Raman scattering in Figure 3B, we see that the intensity of the Raman spectra is diminished. This corroborates our previous conclusion that Raman excited molecules change the interparticle distance. As the distance changes, the plasmon resonance and the laser become detuned, the interparticle hot spot becomes less "hot", and therefore Raman activity subsides. Let us first consider the case where both decreasing Raman activity and a distance change are detected. In this case, the protein that governs the interparticle distance is situated entirely or, more likely, partly in the interparticle hot spot (Figure 3d). When the dimer is exposed to on-axis-polarized light of the correct frequency, a huge enhancement of the electric field can lead to a population of vibrational levels of the molecules in the hot spot.[10] The excitation of mechanical degrees of freedom will eventually lead to conformational changes of the protein.[23] In turn, the conformational change of the protein leads to an increase or decrease in the interparticle distance because the protein is the building block that governs this distance (Figure 3d). This process is more likely for larger field enhancement in the interparticle gap. Turning this around, we see that when the dimer assumes a geometry where there is low field enhancement, it is likely to stay in this conformation. This explains both that the plasmon resonance shifts away from the laser frequency and that the average Raman signal becomes weaker over time.

In the case where no Raman signal is detected, the protein linking the particles lies outside the hot spot (Figure 4d). The protein does not experience a field enhancement and thus it is not vibrationally excited either, and therefore it neither produces a measurable Raman signal nor provokes a change in the interparticle distance. A similar scenario applies when the laser light is polarized perpendicular to the dimer axis and therefore cannot induce a large electric field in the interparticle gap (Figure 4e−g). The protein may be located in the interparticle gap, but the molecule experiences only a weak electric field, and neither a Raman signal nor a change in inter-nanoparticle distance is observed.

We have considered several alternative explanations for the movement of the nanoparticles, but none of them can explain the observations satisfactorily. First, it might be assumed that the absorption of light energy by the nanoparticles in the focused laser beam causes them to melt or at least to heat up their environment and thermally induce a change in protein conformation. Most importantly, this model would not explain the observed correlation between Raman scattering and plasmon shift. Moreover, we have carried out a finite-element calculation of heat dissipation from the nanoparticle dimer to its aqueous environment and obtain an increase of about 3 K for a laser intensity of 50 $\mu W/\mu m^2$ (cf. Supporting Information). A temperature of 3 K above room temperature is not sufficient to melt the particles or to induce protein unfolding. Reported forces for protein unfolding are on the order of 10 pN and above.[24−26] A stretching of 1 nm (Figure 3a,c) thus requires an energy of at least 125 meV, about five times as much as the thermal energies in our experiment. However, the typical observed Raman shift is about 1500 cm^{-1} (Figure 3b), meaning that each Raman scattered photon deposits a vibrational energy $E_{vib} = 186$ meV.

Second, the distance change might be brought about by strong optical forces arising from field gradients in the hot spot.[27,28] However, if optical forces were responsible for the distance changes, such distance changes would be observed for all dimers including those that do not show a Raman signal. This is not the case: distance changes are only observed when there is Raman activity (Figure 5).

Our finding that Raman-excited molecules act back on the geometry and the resonances of a SERS substrate is of general significance for the design and understanding of SERS sensors. It needs to be considered as an alternative explanation or as an additional source of blinking, spectral jumping, and bleaching in SERS experiments and applications. It is also important for the dynamics of self-adaptive metal−nanoparticle SERS substrates.[29] Apart from that, the effect that the plasmon resonance shifts away from the Raman laser might be exploited in design of spectral filters containing metal nanostructures, with laser light of lower intensity than hitherto used.[30,31] This would allow construction of saturable absorbers and optical filters whose spectral region of transparency can be switched by low-intensity laser illumination.

In conclusion, we have shown that Raman-excited protein linkers between two nanoparticles change the inter-nanoparticle distance. When the linker protein is exposed to the strongly enhanced electric field in the interparticle hot spot, the protein actively alters this hot spot. Our results can be explained by vibrational excitation of the protein, which leads to a change of its conformation that pushes the nanoparticles apart or pulls them together. This process continues until a conformation is reached where the coupled plasmon is no longer in resonance with the Raman laser.

The system studied in this report thus "avoids" the exciting field mostly in the spectral domain. In spectrally less sensitive systems one can imagine this avoiding to become mainly spatial in nature. Here, SERS-induced motion of the Raman-active molecules might continue until they are finally spatially driven out of the hot spot.

Acknowledgment. We thank Werner Stadler and Anna Helfrich for excellent technical assistance and Dr. Martin Schlapschy for initial help with gel electrophoresis. This work has been supported by the Deutsche Forschungsgemeinschaft (DFG) through the SFB 486, by the Gottfried-Wilhelm-Leibniz Program, and by the Bavarian Science Foundation. Financial support of the German Excellence Initiative via the "Nanosystems Initiative Munich (NIM)" is gratefully acknowledged.

Supporting Information Available: Figures showing calculation of the optical heating. This material is available free of charge via the Internet at http://pubs.acs.org.

References

(1) Fleischmann, M.; Hendra, P. J.; McQuillan, A. J. *Chem. Phys. Lett.* **1974**, *26*, 163.
(2) Albrecht, M. G.; Creighton, J. A. *J. Am. Chem. Soc.* **1977**, *99*, 5215.
(3) Jeanmaire, D. L.; Van Duyne, R. P. *J. Electroanal. Chem.* **1977**, *84*, 1.
(4) Kneipp, K.; et al. *Phys. Rev. E* **1998**, *57*, R6281.
(5) Cao, Y. C.; Jin, R.; Mirkin, C. A. *Science* **2002**, *297*, 1536.
(6) Ahern, A. M.; Garrell, R. L. *Langmuir* **1991**, *7*, 254.
(7) Xu, H.; Bjerneld, E. J.; Käll, M.; Börjesson, L. *Phys. Rev. Lett.* **1999**, *83*, 4357.
(8) Kneipp, K.; et al. *Phys. Rev. Lett.* **1997**, *78*, 1667.
(9) Nie, S.; Emory, S. R. *Science* **1997**, *275*, 1102.
(10) Kneipp, K.; et al. *Phys. Rev. Lett.* **1996**, *76*, 2444.
(11) Pockrand, I.; Billmann, J.; Otto, A. *J. Chem. Phys.* **1983**, *78*, 6384.
(12) Moskovits, M. *J. Chem. Phys.* **1978**, *69*, 4159.
(13) Le Ru, E. C.; Etchegoin, P. G.; Meyer, M. *J. Chem. Phys.* **2006**, *125*, 204701.
(14) Xu, H.; Käll, M. *ChemPhysChem* **2003**, *4*, 1001.
(15) Talley, C. E.; Jackson, J. B.; Oubre, C.; Grady, N. K.; Hollars, C. W.; Lane, S. M.; Huser, T. R.; Nordlander, P.; Halas, N. J. *Nano Lett.* **2005**, *5*, 1569.
(16) Quinten, M.; Kreibig, U.; Schönauer, D.; Genzel, L. *Surf. Sci.* **1985**, *156*, 741.
(17) Sönnichsen, C.; Reinhard, B. M.; Liphardt, J.; Alivisatos, A. P. *Nat. Biotechnol.* **2005**, *23*, 741.
(18) Sönnichsen, C.; et al. *Phys. Rev. Lett.* **2002**, *88*, 077402.
(19) Suh, Y. D.; Schenter, G. K.; Zhu, L.; Lu, H. P. *Ultramicroscopy* **2003**, *97*, 89.
(20) Nordlander, P.; Oubre, C.; Prodan, E.; Li, K.; Stockman, M. I. *Nano Lett.* **2004**, *4*, 899.
(21) Tamaru, H.; Kuwata, H.; Miyazaki, H. T.; Miyano, K. *Appl. Phys. Lett.* **2002**, *80*, 1826.
(22) Sasic, S.; Itoh, T.; Ozaki, Y. *J. Raman Spectrosc.* **2005**, *36*, 593.
(23) Dian, B. C.; Longarte, A.; Zwier, T. S. *Science* **2002**, *296*, 2369.
(24) Rief, M.; Gautel, M.; Oesterhelt, F.; Fernandez, J. M.; Gaub, H. E. *Science* **1997**, *276*, 1109.
(25) Tskhovrebova, L.; Trinick, J.; Sleep, J. A.; Simmons, R. M. *Nature* **1997**, *387*, 308.
(26) Kellermayer, M. S. Z.; Smith, S. B.; Granzier, H. L.; Bustamante, C. *Science* **1997**, *276*, 1112.
(27) Xu, H.; Käll, M. *Phys. Rev. Lett.* **2002**, *89*, 246802.
(28) Fuchs, R.; Claro, F. *Appl. Phys. Lett.* **2004**, *85*, 3280.
(29) Drachev, V. P.; Nashine, V. C.; Thoreson, M. D.; Ben-Amotz, D.; Davisson, V. J.; Shalaev, V. M. *Langmuir* **2005**, *21*, 8368.
(30) Vollmer, M.; Weidenauer, R.; Hoheisel, W.; Schulte, U.; Träger, F. *Phys. Rev. B* **1989**, *40*, 12509.
(31) Genov, D. A.; Sarychev, A. K.; Shalaev, V. M. *J. Nonlinear Opt. Phys. Mater.* **2003**, *12*, 419.

NL0712466